Particle size monitoring of $BaCl_2$ nanocrystals in fluorozirconate glasses

U. Skrzypczak[a,*], C. Pfau[a], C. Bohley[a], G. Seifert[a,b], S. Schweizer[b,c]

[a] *Centre for Innovation Competence SiLi-nano®, Martin Luther University of Halle-Wittenberg, Karl-Freiherr-von-Fritsch-Str. 3, 06120 Halle (Saale), Germany*
[b] *Fraunhofer Center for Silicon Photovoltaics CSP, Walter-Hülse-Str. 1, 06120 Halle (Saale), Germany*
[c] *Department of Electrical Engineering, South Westphalia University of Applied Sciences, Lübecker Ring 2, 59494 Soest, Germany*

Abstract

Thermal processing of fluorochlorozirconate glasses leads to the formation of $BaCl_2$ nanocrystals within the glass matrix. An alternative method to determine the size of the nanocrystals is provided by a Rayleigh scattering model based analysis of optical transmittance data. For comparison, the size is extracted from X-ray diffraction data with the Scherrer equation. Additional unwanted inclusions of non-crystalline scattering centers lead to significant differences between the results obtained from both of these techniques. Using these two methods allows for a controlled monitoring of nanocrystal growth in optical materials.

Keywords: Diffraction and scattering, X-ray diffraction, Nanocrystals
PACS: 42.25.Fx, 61.05.cp, 78.20.Bh, 78.67.Bf

1. Introduction

Photonic glasses doped with rare-earth ions such as Er^{3+}, Nd^{3+}, Yb^{3+}, and Eu^{2+} have gathered significant interest due to their possible application in fiber lasers, frequency conversion devices or as luminophores for ionizing radiation to name only a few [1, 2]. As such they are better suited than other candidates due to their high optical transparency over a broad wavelength range. The inclusion of nanoparticles from low phonon energy materials inside such glasses allows for a significant improvement of the luminescence properties of the rare-earths by a strong reduction of losses to multiphonon relaxation [3, 4]. As shown previously [5], a uniform growth of $BaCl_2$ nanocrystals inside such glasses can be induced with thermal treatment if additional chlorine is introduced at the expense of fluoride. Moreover, certain rare-earths including Nd^{3+} tend to improve the crystallization, acting as a nucleation seed [6].

X-ray diffraction and the Scherrer formula as well as transmission electron microscopy are known techniques for the determination of nanocrystal sizes. Howoever, since the nanocrystal growth also affects the optical behavior of the samples, a size analysis from fitting a Rayleigh scattering model to transmittance baseline data is presented as an interesting alternative tothese established tools.

The average sizes of $BaCl_2$ nanocrystals grown in fluorochlorozirconate (FCZ) glass matrices by different thermal treatment temperatures were studied. They were determined employing X-ray diffraction and the Scherrer equation. In addition, an alternative measure of the crystal sizes was obtained from an analysis based on Rayleigh scattering at the nanocrystals. From the relation between the results obtained from the two methods, a way to monitor a production optimization towards high optical quality samples is proposed.

2. Materials and methods

The FCZ glass samples investigated are comprised of $52ZrF_4$–$10BaF_2$–$10BaCl_2$–$19NaCl$–$3.5LaF_3$–$3AlF_3$–$0.5InF_3$–$1KCl$–$1NdF_3$ (values in mol%). The constituent chemicals were melted in a glassy carbon crucible at 745 °C in an inert atmosphere and then poured into a brass mold that was at a temperature of 200 °C, before being slowly cooled to room temperature. The FCZ glasses were subsequently treated thermally under an inert atmosphere at a temperature between 240 °C and 290 °C for 20 min to initiate the formation of $BaCl_2$ nanocrystals therein. Differential scanning calorimetry showed that the formation of $BaCl_2$ nanocrystals occurs in the temperature range between 260 and 290 °C which is above the glass transition temperature T_g of 210 °C [7].

Two different glass series, denoted as sample series #1 and #2, were prepared. During the preparation of sample series #1, special attention was paid to achieve high optical quality by using only new, highly pure and finely powdered materials. Inclusions and bubbles were avoided by using a fast pour-out method. The visual appearances of the as-made glass and the samples heat treated at 240 °C to 270 °C were transparent. Those heat-treated at 280 °C and 290 °C looked milky white in both series. Overall, sample series #1 appeared more transparent and was of better optical quality.

X-ray diffraction (XRD) measurements were performed in Bragg-Brentano focusing geometry using copper K_α radiation from an AXS D8 Advance diffractometer (Bruker) operating at 40 kV and 40 mA. Transmission spectra were recorded from 200 nm to 900 nm with a UV/Vis/NIR spectrophotometer (Perkin Elmer Lambda 1050) coupled to a 150 mm integrating sphere.

*Corresponding author
Email address: ulrich.skrzypczak@physik.uni-halle.de (U. Skrzypczak)

3. Results and discussion

3.1. X-ray diffraction

Figure 1 (a) shows a typical XRD pattern for a fluorozirconate-based glass containing hexagonal $BaCl_2$ nanocrystals [8]. The as-made glass, which does not show any crystalline phases, was thermally treated at 260 °C for 20 min leading to the formation of hexagonal phase $BaCl_2$ nanocrystals (space group $P\bar{6}2m$ (189)) therein [9]. The bar pattern shows the corresponding powder diffraction data (PDF entry #45-1313) for comparison. The amorphous background is the contribution of the glass. Up to treatment temperatures of 260 °C only reflections related to hexagonal $BaCl_2$ are detectable, whereas a phase transition to the orthorhombic $BaCl_2$ structure (space group *Pnma* (62)) can be observed upon thermal treatment at temperatures higher than 270 °C (data not shown) [8]. To allow for an unambiguous identification of the various reflections, in particular in the case of mixed phases, the XRD pattern for hexagonal and orthorhombic phase $BaCl_2$ were calculated [10] using crystallographic parameters from Haase et al. [11], which have been theoretically confirmed by Bohley et al. [12] recently. The calculated data for hexagonal $BaCl_2$ are shown in Figure 1 (b).

One method of size determination of the nanoparticles is based on the Scherrer formula [13] and calculated from the linewidth of the most intense XRD reflection. However, for this way of particle size analysis two things have to be considered: Firstly, the accuracy of such a single-reflection size analysis can be low. Secondly, and more generally, only a value near to the average particle size is obtained since the assumption of spherical particle shapes is often not justified. For non-spherical objects, however, a single XRD peak is related to the extension of the nanoparticle along a certain spatial direction, and therefore the result could be significantly smaller than its actual size [13, 14].

In order to achieve better accuracy, for each observed reflection, j, with a relative intensity of more than 20% of the respective phase's maximum, the diffraction angle, ϑ_j, as well as the corresponding full-width at half-maximum, $\Delta\vartheta_j$, was determined for reflections that do not interfere with each other (see Figure 1 (b)). Subsequently, the Scherrer formula [13]

$$d_{hkl} = \frac{K\lambda}{\Delta\vartheta_j \cos\vartheta_j} \tag{1}$$

was used to determine the corresponding nanocrystal diameter. Here, d_{hkl} is the nanocrystal size in the direction perpendicular to the lattice planes with Miller indices hkl, ϑ_j the Bragg angle, and $\lambda = 1.5418$ Å the wavelength of the X-rays. The crystallite-shape factor, K, in (1) was set to 0.9, the most suitable approximation when detailed shape information is not available [14]; stress and strain effects were neglected. A Lorentzian line profile was used in the fitting procedure.

The d_{hkl} values were then averaged over all analyzed reflections per sample and the resulting mean value is taken as the nanocrystal size. However, this value must still be treated as a rough estimate of the average nanocrystal size. Furthermore, this way of size determination by using the Scherrer formula is usually only applied to spherical nanoparticles smaller than 100 nm [14]. Table 1 outlines the XRD linewidth analysis for the two different sample series.

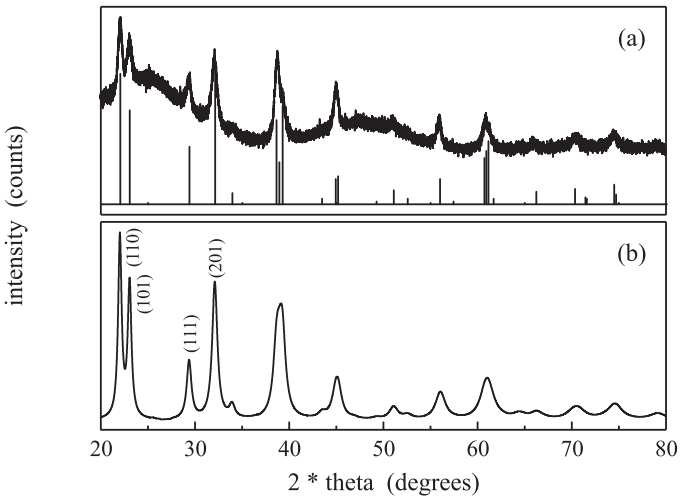

Figure 1: (a) XRD data of a fluorozirconate-based glass containing hexagonal phase $BaCl_2$ nanocrystals (Series #1, 260 °C). In addition to the sharp reflections from $BaCl_2$, the data show the amorphous background from the glass matrix. The powder diffraction data of hexagonal $BaCl_2$ (PDF #45-1313) is shown for comparison. (b) Calculated XRD pattern for hexagonal phase $BaCl_2$ nanocrystals with a particle size of 25 nm; for the calculation a Lorentzian line profile was used. The Miller indices of the peaks used for particle size estimation are indicated in the figure.

Table 1: Overview on the particle size analysis.

treatment	particle sizes (nm)			
temp. (°C)	XRD #1	Rayleigh #1	XRD #2	Rayleigh #2
240	12	12	13	13
250	13	14	15	34
260	19	25	23	61
270	45	42	40	73
280	61	65	67	-
290	73	80	80	-

3.2. Optical spectroscopy

Optical absorption spectra were measured for a series of samples with different thermal treatment temperatures and hence different nanocrystal sizes. In Figure 2 the significant increase in Rayleigh scattering with increasing nanocrystal size can be observed by the dramatic decrease of the transmission baseline. The spectral features (absorption bands) are caused by transitions from the Nd^{3+} ground state $^4I_{9/2}$ to several excited $4f$ states. See Stanley et al. [15] for further details on the Nd^{3+}-related transitions in fluorozirconate-based glasses. It has been verified with measurements utilizing an integrating sphere that the baseline of the transmittance spectra originates from scattering only and that no additional absorption has been induced by the thermal treatment.

The observed scattering of light in the visible and near infrared spectral range provides an alternative approach to deter-

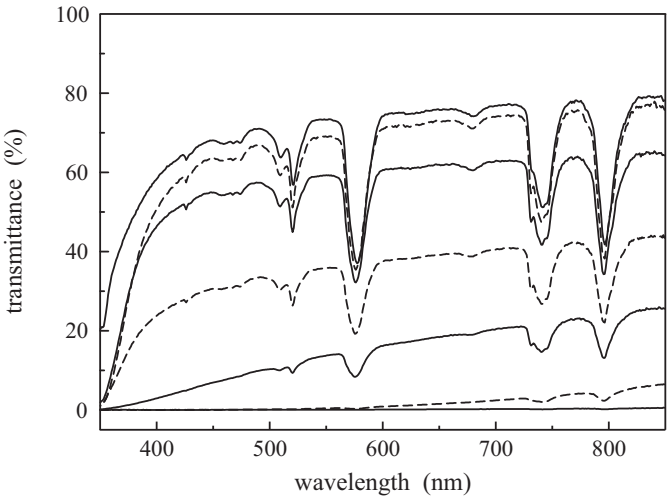

Figure 2: Transmittance spectra for Nd^{3+}-doped fluorozirconate-based glasses containing $BaCl_2$ nanocrystals of different sizes; the sample thickness was 1.6 mm. To initiate the formation of the $BaCl_2$ nanocrystals, the as-made glass (top curve) was thermally treated at temperatures of 240 °C, 250 °C, 260 °C, 270 °C, 280 °C, and 290 °C (from top to bottom).

mine the size of the $BaCl_2$ nanocrystals in the glass matrix. Not only crystalline, but any inclusion with a refractive index other than that of the matrix, contributes to the scattering intensity. For the Rayleigh scattering analysis conducted in the following, the transmission spectra shown in Figure 2 were corrected for the reflection at the sample surfaces. The baselines of the resulting extinction curves (Nd^{3+} absorption features excluded) were fitted in the spectral range from 400 nm to 800 nm with a Mie scattering model in the Rayleigh limit [16] including inter-particle interference effects [17] instead of independent Rayleigh scatterers [18]. Accordingly, nanoparticle scattering is described by an extinction coefficient of the form

$$\alpha_{\text{Rayleigh}}(\lambda) = 4\pi^4\delta_i(1-\delta_i)d^3\left(\frac{(n_i(\lambda)/n_m(\lambda))^2-1}{(n_i(\lambda)/n_m(\lambda))^2+2}\right)^2\left(\frac{n_m(\lambda)}{\lambda}\right)^4 \quad (2)$$

where δ_i is the volume fraction of the scattering particle, d its diameter, and n_i and n_m are the refractive indices of particle inclusion and matrix, respectively [19, 20]. The volume fractions of the crystallites were estimated from the ratio of the crystalline peak area of hexagonal $BaCl_2$ and the total XRD graph area [21] assuming comparable X-ray absorption properties of the different materials and phases.

The results are comparable to values determined elsewhere [22] and are summarized in Table 2. As shown there, the volume fractions are mostly in the range of the maximum possible volume fraction of approximately 20%, which is the limit given by the mole-fraction of $BaCl_2$ included into the samples. The lower temperature samples have lower values indicating that not all Cl^- ions are used up to form $BaCl_2$ nanocrystals yet. The fact that the volume fraction is staying almost constant for higher treatment temperatures, while the particle sizes rise, shows that initially small nanoparticles grow independently in the lower temperature ranges and the growth proceeds from the precipitation of small hexagonal crystals through Ostwald

Table 2: Volume fractions as determined from XRD.

treatment	volume fractions (%)	
temperature (°C)	Series #1	Series #2
240	16	14
250	16	15
260	19	17
270	18	20
280	15	17

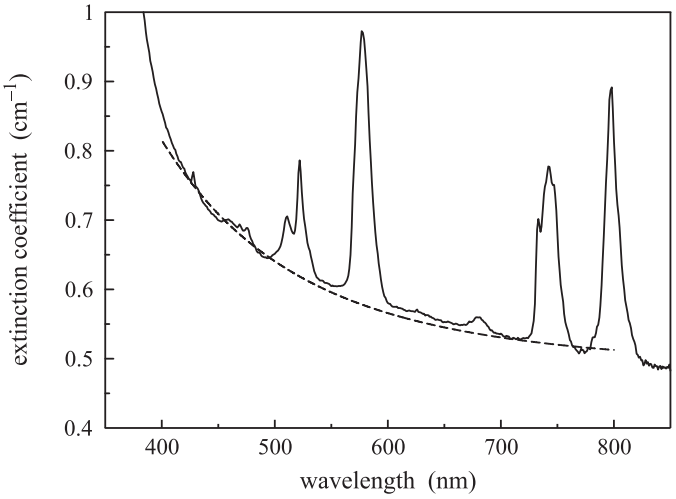

Figure 3: Fit (dashed curve) for the extinction coefficient of an FCZ glass ceramic containing 20 vol.% $BaCl_2$ nanoparticles with an average size of 25 nm.

ripening [23]: small particles dissolve, and the larger ones will grow from this fresh nutrient until they reach their final size, minimizing the total surface energy. The volume fractions for the 290 °C sample could not be analyzed as partial glass crystallization prevents a clear reflection assignment. Figure 3 shows a fit for the extinction coefficient of an FCZ glass ceramic containing 20 vol.% $BaCl_2$ nanoparticles with an average size of 25 nm. Edgar et al. [18] applied the Rayleigh scattering only to the spectral range between 400 nm and 600 nm due to strong disturbances from macroscopic defects such as bubbles in the remaining range. For the study presented here, the fitting works well up to 800 nm. A better sample quality lacking such inclusions could be one reason.

3.3. Particle size analysis – Rayleigh scattering versus X-ray diffraction

To evaluate the influence of unwanted inclusions, another sample series with apparently worse optical quality was measured and analyzed; these samples were prepared with the same compositional parameters but under different preparation conditions. Figure 4 shows the respective crystal sizes for the two sample series determined both with the Rayleigh and the XRD/Scherrer method. For the sample series with better optical quality (denoted series #1) the sizes obtained from either method correspond very well. The sizes determined via XRD from the sample series of slightly worse optical quality

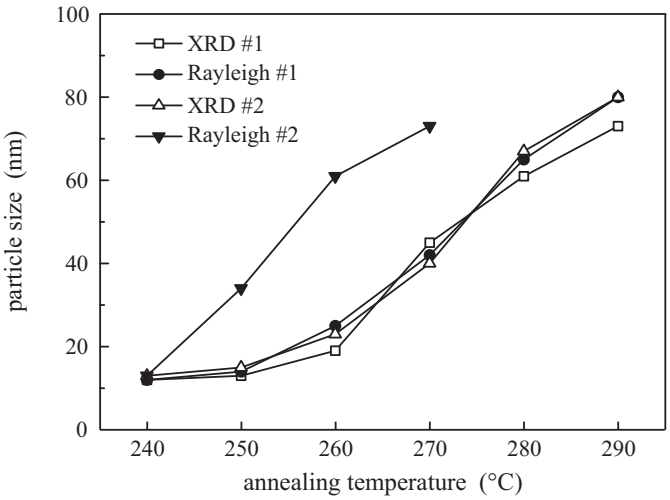

Figure 4: Particle size analysis using Rayleigh scattering and X-ray diffraction for sample series #1 and #2.

(denoted series #2) are also very similar which implicates that crystal growth is reproducibly stable under the given preparation conditions. The sizes derived from the Rayleigh method, however, do not reproduce the XRD values for this sample series, but exceed them by a factor of two to three depending on the thermal treatment temperature. Obviously, additional non-crystalline inclusions are being created in these samples leading to increased scattering intensity. The spectra corresponding to treatment temperatures above 270 °C could not be analyzed since scattering was too strong.

To identify the origin of these additional inclusions, the experimental trends have to be considered. Similar to the nanocrystals, the non-crystalline inhomogeneities grow in size with increasing thermal treatment temperature. Yet, the growth is apparently much faster, as the larger slope of size versus thermal treatment temperature clearly indicates. Gas bubbles could be a possible explanation for such fast-growing inclusions. These bubbles, in turn, would be probable in case of water inclusions in the FCZ glass. Despite the water-free inert gas production environment, a small amount of water could have entered the samples after the production process eventually leading to the formation of the two $BaCl_2$ hydrates $BaCl{\cdot}2H_2O$ and $BaCl{\cdot}1H_2O$ [11]. To obtain an estimate of the amount of possible unwanted water inclusions in the samples, a ^{1}H-nuclear magnetic resonance experiment has been carried out. The relative intensities of the ^{1}H-NMR-signals from the glass ceramic and a polybutadiene reference sample yielded a ^{1}H concentration of 6.48 mmol%, several orders of magnitude lower than the $BaCl_2$ concentration and hence too small to account for the considerable effect observed in the samples.

Unfortunately, it cannot be decided at this point, whether the additional scattering centers are caused by gas bubbles of a different chemical origin or whether an unexpected demixing of some glass components might have been occurred. Further investigations will be necessary to answer that question.

Irrespective of this point, the observations in this work demonstrate that a comparison of the sizes of nanometric scatterers determined either by the Rayleigh scattering method or the XRD/Scherrer method allows for an estimate of the amount of unwanted, non-crystalline scattering inclusions. Evaluating the difference between the XRD- and scattering-determined nanocrystal sizes appears to be an attractive approach able to monitor how a change in the preparation procedure affects the quality of the sample, and thereby allows for an optimization of the sample with respect to production for high optical quality. It is noteworthy that this procedure can also be applied to samples consisting of several types of crystalline nano-inclusions. Here, the average size of each particular inclusion type can be determined separately with XRD and the Scherrer formula. From the difference between the corresponding sizes obtained here and from the Rayleigh approach, the influence of the undesired scatterers can be deduced.

4. Conclusion

Nanocrystal size analysis by a parametric fit of a Rayleigh scattering model to transmittance data is presented here as an alternative to established methods of size characterization such as XRD and TEM. $BaCl_2$ nanocrystals grown to different average sizes inside an FCZ glass matrix were analyzed by applying X-ray diffraction and the Scherrer equation. In comparison, the crystal sizes were obtained from the Rayleigh scattering method. The results correspond very well. Since additional inclusions of non-crystalline scattering centers change the relation between the results obtained from either of the two techniques, a qualitative method of monitoring a production optimization towards production of high optical quality samples is obtained.

Acknowledgments

This work was supported by the FhG Internal Programs under Grant No. Attract 692 034. In addition, the authors would like to thank the Federal Ministry for Education and Research ("Bundesministerium für Bildung und Forschung") for their financial support within the Centre for Innovation Competence SiLi-nano® (Project No. 03Z2HN11). We also thank Bernd Ahrens for providing samples, Frank Lange for the NMR measurement and Franziska Steudel for helpful discussions.

[1] J. A. Johnson, S. Schweizer, B. Henke, G. Chen, J. Woodford, P. J. Newman, and D. R. MacFarlane, J. Appl. Phys. 100 (2006) 034701.
[2] J. A. Johnson, S. Schweizer, and A. R. Lubinsky, J. Am. Ceram. Soc. 90 (2007) 693.
[3] U. Skrzypczak, M. Miclea, A. Stalmashonak, B. Ahrens, B. Henke, G. Seifert, J. A. Johnson, and S. Schweizer, Phys. Status Solidi C 8, 2649 (2011) 2649.
[4] C. Pfau, C. Bohley, P.-T. Miclea, and S. Schweizer, J. Appl. Phys. 109 (2011) 083545.
[5] B. Ahrens, P. Löper, J. C. Goldschmidt, S. Glunz, B. Henke, P.-T. Miclea, and S. Schweizer, Phys. Status Solidi A 205 (2008) 2822.
[6] C. Paßlick, B. Ahrens, B. Henke, J. A. Johnson, and S. Schweizer, J. Non-Cryst. Sol. 357 (2011) 2450.
[7] B. Ahrens, C. Eisenschmidt, J. A. Johnson, P. T. Miclea, and S. Schweizer, Appl. Phys. Lett. 92 (2008) 061905.
[8] C. Pfau, U. Skrzypczak, M. Miclea, C. Bohley, P.-T. Miclea, and S. Schweizer, MRS Proceedings 1404 (2012) mrsf11-1404-w02-10.
[9] G. Liu and H. A. Eick, J. Less-Common Met. 149 (1989) 47.

[10] W. Kraus and G. Nolze, J. Appl. Cryst. 29 (1996) 301.
[11] A. Haase and G. Brauer, Z. Anorg. Allg. Chem. 441 (1978) 181.
[12] C. Bohley, J.-M. Wagner, C. Pfau, P.-T. Miclea, and S. Schweizer, Phys. Rev. B 83 (2011) 024107.
[13] P. Scherrer, Göttinger Nachrichten Math. Phys. 2 (1918) 1.
[14] U. Holzwarth and N. Gibson, Nat. Nano. 6 (2011) 534.
[15] A. T. Stanley, E. A. Harris, T. M. Searle, and J. M. Parker, J. Non-Cryst. Solids 161 (1993) 235.
[16] C. F. Bohren and D. R. Huffmann, Absorption and Scattering of Light by Small Particles, 1st ed., Wiley, New York, 1983.
[17] M. Shepilov, Opt. Mat. 30 (2008) 839.
[18] A. Edgar, G. V. M. Williams, and J. Hamelin, Curr. Appl. Phys. 6 (2006) 355.
[19] H. H. Li, J. Phys. Chem. Ref. Data 9 (1980) 161.
[20] L. Wetenkamp, T. Westendorf, G. West, and A. Kober, Mater. Sci. Forum 32-33 (1991) 471.
[21] T. Gloriant, M. Gich, S. Suriñach, M. D. Baró, and A. L. Greer, Mater. Sci. Forum 343-346 (2000) 365.
[22] S. Schweizer, L. W. Hobbs, M. Secu, J.-M. Spaeth, and A. Edgar, J. Appl. Phys. 97 (2005) 083522.
[23] J. W. Dunning and A. L. Smith, Particle Growth in Suspension, 1st ed., Academic Press, London, 1973.